J/ψ Production versus Transverse Momentum and Rapidity in $p + p$ Collisions at $\sqrt{s} = 200$ GeV

A. Adare,[8] S. Afanasiev,[22] C. Aidala,[9] N. N. Ajitanand,[48] Y. Akiba,[42,43] H. Al-Bataineh,[37] J. Alexander,[48] K. Aoki,[27,42] L. Aphecetche,[50] R. Armendariz,[37] S. H. Aronson,[3] J. Asai,[43] E. T. Atomssa,[28] R. Averbeck,[49] T. C. Awes,[38] B. Azmoun,[3] V. Babintsev,[18] G. Baksay,[14] L. Baksay,[14] A. Baldisseri,[11] K. N. Barish,[4] P. D. Barnes,[30] B. Bassalleck,[36] S. Bathe,[4] S. Batsouli,[38] V. Baublis,[41] A. Bazilevsky,[3] S. Belikov,[3] R. Bennett,[49] Y. Berdnikov,[45] A. A. Bickley,[8] J. G. Boissevain,[30] H. Borel,[11] K. Boyle,[49] M. L. Brooks,[30] H. Buesching,[3] V. Bumazhnov,[18] G. Bunce,[3,43] S. Butsyk,[30,49] S. Campbell,[49] B. S. Chang,[57] J.-L. Charvet,[11] S. Chernichenko,[18] J. Chiba,[23] C. Y. Chi,[9] M. Chiu,[19] I. J. Choi,[57] T. Chujo,[54] P. Chung,[48] A. Churyn,[18] V. Cianciolo,[38] C. R. Cleven,[16] B. A. Cole,[9] M. P. Comets,[39] P. Constantin,[30] M. Csanád,[13] T. Csörgő,[24] T. Dahms,[49] K. Das,[15] G. David,[3] M. B. Deaton,[1] K. Dehmelt,[14] H. Delagrange,[50] A. Denisov,[18] D. d'Enterria,[9] A. Deshpande,[43,49] E. J. Desmond,[3] O. Dietzsch,[46] A. Dion,[49] M. Donadelli,[46] O. Drapier,[28] A. Drees,[49] A. K. Dubey,[56] A. Durum,[18] V. Dzhordzhadze,[4] Y. V. Efremenko,[38] J. Egdemir,[49] F. Ellinghaus,[8] W. S. Emam,[4] A. Enokizono,[29] H. En'yo,[42,43] S. Esumi,[53] K. O. Eyser,[4] D. E. Fields,[36,43] M. Finger,[5,22] M. Finger, Jr.,[5,22] F. Fleuret,[28] S. L. Fokin,[26] Z. Fraenkel,[56] J. E. Frantz,[49] A. Franz,[3] A. D. Frawley,[15] K. Fujiwara,[42] Y. Fukao,[27,42] T. Fusayasu,[35] S. Gadrat,[31] I. Garishvili,[51] A. Glenn,[8] H. Gong,[49] M. Gonin,[28] J. Gosset,[11] Y. Goto,[42,43] R. Granier de Cassagnac,[28] N. Grau,[21] S. V. Greene,[54] M. Grosse Perdekamp,[19,43] T. Gunji,[7] H.-Å. Gustafsson,[32] T. Hachiya,[17] A. Hadj Henni,[50] C. Haegemann,[36] J. S. Haggerty,[3] H. Hamagaki,[7] R. Han,[40] H. Harada,[17] E. P. Hartouni,[29] K. Haruna,[17] E. Haslum,[32] R. Hayano,[7] M. Heffner,[29] T. K. Hemmick,[49] T. Hester,[4] X. He,[16] H. Hiejima,[19] J. C. Hill,[21] R. Hobbs,[36] M. Hohlmann,[14] W. Holzmann,[48] K. Homma,[17] B. Hong,[25] T. Horaguchi,[42,52] D. Hornback,[51] T. Ichihara,[42,43] K. Imai,[27,42] M. Inaba,[53] Y. Inoue,[44,42] D. Isenhower,[1] L. Isenhower,[1] M. Ishihara,[42] T. Isobe,[7] M. Issah,[48] A. Isupov,[22] B. V. Jacak,[49] J. Jia,[9] J. Jin,[9] O. Jinnouchi,[43] B. M. Johnson,[3] K. S. Joo,[34] D. Jouan,[39] F. Kajihara,[7] S. Kametani,[7,55] N. Kamihara,[42] J. Kamin,[49] M. Kaneta,[43] J. H. Kang,[57] H. Kanou,[42,52] D. Kawall,[43] A. V. Kazantsev,[26] A. Khanzadeev,[41] J. Kikuchi,[55] D. H. Kim,[34] D. J. Kim,[57] E. Kim,[47] E. Kinney,[8] A. Kiss,[13] E. Kistenev,[3] A. Kiyomichi,[42] J. Klay,[29] C. Klein-Boesing,[33] L. Kochenda,[41] V. Kochetkov,[18] B. Komkov,[41] M. Konno,[53] D. Kotchetkov,[4] A. Kozlov,[56] A. Král,[10] A. Kravitz,[9] J. Kubart,[5,20] G. J. Kunde,[30] N. Kurihara,[7] K. Kurita,[44,42] M. J. Kweon,[25] Y. Kwon,[51,57] G. S. Kyle,[37] R. Lacey,[48] Y.-S. Lai,[9] J. G. Lajoie,[21] A. Lebedev,[21] D. M. Lee,[30] M. K. Lee,[57] T. Lee,[47] M. J. Leitch,[30] M. A. L. Leite,[46] B. Lenzi,[46] T. Liška,[10] A. Litvinenko,[22] M. X. Liu,[30] X. Li,[6] B. Love,[54] D. Lynch,[3] C. F. Maguire,[54] Y. I. Makdisi,[3] A. Malakhov,[22] M. D. Malik,[36] V. I. Manko,[26] Y. Mao,[40,42] L. Mašek,[5,20] H. Masui,[53] F. Matathias,[9] M. McCumber,[49] P. L. McGaughey,[30] Y. Miake,[53] P. Mikeš,[5,20] K. Miki,[53] T. E. Miller,[54] A. Milov,[49] S. Mioduszewski,[3] M. Mishra,[2] J. T. Mitchell,[3] M. Mitrovski,[48] A. Morreale,[4] D. P. Morrison,[3] T. V. Moukhanova,[26] D. Mukhopadhyay,[54] J. Murata,[44,42] S. Nagamiya,[23] Y. Nagata,[53] J. L. Nagle,[8] M. Naglis,[56] I. Nakagawa,[42,43] Y. Nakamiya,[17] T. Nakamura,[17] K. Nakano,[42,52] J. Newby,[29] M. Nguyen,[49] B. E. Norman,[30] A. S. Nyanin,[26] E. O'Brien,[3] S. X. Oda,[7] C. A. Ogilvie,[21] H. Ohnishi,[42] H. Okada,[27,42] K. Okada,[43] M. Oka,[53] O. O. Omiwade,[1] A. Oskarsson,[32] M. Ouchida,[17] K. Ozawa,[7] R. Pak,[3] D. Pal,[54] A. P. T. Palounek,[30] V. Pantuev,[49] V. Papavassiliou,[37] J. Park,[47] W. J. Park,[25] S. F. Pate,[37] H. Pei,[21] J.-C. Peng,[19] H. Pereira,[11] V. Peresedov,[22] D. Yu. Peressounko,[26] C. Pinkenburg,[3] M. L. Purschke,[3] A. K. Purwar,[30] H. Qu,[16] J. Rak,[36] A. Rakotozafindrabe,[28] I. Ravinovich,[56] K. F. Read,[38,51] S. Rembeczki,[14] M. Reuter,[49] K. Reygers,[33] V. Riabov,[41] Y. Riabov,[41] G. Roche,[31] A. Romana,[28,*] M. Rosati,[21] S. S. E. Rosendahl,[32] P. Rosnet,[31] P. Rukoyatkin,[22] V. L. Rykov,[42] B. Sahlmueller,[33] N. Saito,[27,42,43] T. Sakaguchi,[3] S. Sakai,[53] H. Sakata,[17] V. Samsonov,[41] S. Sato,[23] S. Sawada,[23] J. Seele,[8] R. Seidl,[19] V. Semenov,[18] R. Seto,[4] D. Sharma,[56] I. Shein,[18] A. Shevel,[41,48] T.-A. Shibata,[42,52] K. Shigaki,[17] M. Shimomura,[53] K. Shoji,[27,42] A. Sickles,[49] C. L. Silva,[46] D. Silvermyr,[38] C. Silvestre,[11] K. S. Sim,[25] C. P. Singh,[2] V. Singh,[2] S. Skutnik,[21] M. Slunečka,[5,22] A. Soldatov,[18] R. A. Soltz,[29] W. E. Sondheim,[30] S. P. Sorensen,[51] I. V. Sourikova,[3] F. Staley,[11] P. W. Stankus,[38] E. Stenlund,[32] M. Stepanov,[37] A. Ster,[24] S. P. Stoll,[3] T. Sugitate,[17] C. Suire,[39] J. Sziklai,[24] T. Tabaru,[43] S. Takagi,[53] E. M. Takagui,[46] A. Taketani,[42,43] Y. Tanaka,[35] K. Tanida,[42,43] M. J. Tannenbaum,[3] A. Taranenko,[48] P. Tarján,[12] T. L. Thomas,[36] M. Togawa,[27,42] A. Toia,[49] J. Tojo,[42] L. Tomášek,[20] H. Torii,[42] R. S. Towell,[1] V-N. Tram,[28] I. Tserruya,[56] Y. Tsuchimoto,[17] C. Vale,[21] H. Valle,[54] H. W. van Hecke,[30] J. Velkovska,[54] R. Vertesi,[12] A. A. Vinogradov,[26] M. Virius,[10] V. Vrba,[20] E. Vznuzdaev,[41] M. Wagner,[27,42] D. Walker,[49] X. R. Wang,[37] Y. Watanabe,[42,43] J. Wessels,[33] S. N. White,[3] D. Winter,[9] C. L. Woody,[3] M. Wysocki,[8] W. Xie,[43] Y. Yamaguchi,[55] A. Yanovich,[18] Z. Yasin,[4] J. Ying,[16] S. Yokkaichi,[42,43] G. R. Young,[38] I. Younus,[36] I. E. Yushmanov,[26] W. A. Zajc,[9,†] O. Zaudtke,[33] C. Zhang,[38] S. Zhou,[6] J. Zimányi,[24,*] and L. Zolin[22]

(PHENIX Collaboration)

[1]*Abilene Christian University, Abilene, Texas 79699, USA*
[2]*Department of Physics, Banaras Hindu University, Varanasi 221005, India*
[3]*Brookhaven National Laboratory, Upton, New York 11973-5000, USA*
[4]*University of California–Riverside, Riverside, California 92521, USA*
[5]*Charles University, Ovocný trh 5, Praha 1, 116 36 Prague, Czech Republic*
[6]*China Institute of Atomic Energy (CIAE), Beijing, People's Republic of China*
[7]*Center for Nuclear Study, Graduate School of Science, University of Tokyo, 7-3-1 Hongo, Bunkyo, Tokyo 113-0033, Japan*
[8]*University of Colorado, Boulder, Colorado 80309, USA*
[9]*Columbia University, New York, New York 10027, USA,*
and Nevis Laboratories, Irvington, New York 10533, USA
[10]*Czech Technical University, Zikova 4, 166 36 Prague 6, Czech Republic*
[11]*Dapnia, CEA Saclay, F-91191 Gif-sur-Yvette, France*
[12]*Debrecen University, H-4010 Debrecen, Egyetem tér 1, Hungary*
[13]*ELTE, Eötvös Loránd University, H - 1117 Budapest, Pázmány P. s. 1/A, Hungary*
[14]*Florida Institute of Technology, Melbourne, Florida 32901, USA*
[15]*Florida State University, Tallahassee, Florida 32306, USA*
[16]*Georgia State University, Atlanta, Georgia 30303, USA*
[17]*Hiroshima University, Kagamiyama, Higashi-Hiroshima 739-8526, Japan*
[18]*IHEP Protvino, State Research Center of Russian Federation, Institute for High Energy Physics, Protvino 142281, Russia*
[19]*University of Illinois at Urbana-Champaign, Urbana, Illinois 61801, USA*
[20]*Institute of Physics, Academy of Sciences of the Czech Republic, Na Slovance 2, 182 21 Prague 8, Czech Republic*
[21]*Iowa State University, Ames, Iowa 50011, USA*
[22]*Joint Institute for Nuclear Research, 141980 Dubna, Moscow Region, Russia*
[23]*KEK, High Energy Accelerator Research Organization, Tsukuba, Ibaraki 305-0801, Japan*
[24]*KFKI Research Institute for Particle and Nuclear Physics of the Hungarian Academy of Sciences (MTA KFKI RMKI),*
H-1525 Budapest 114, P.O. Box 49, Budapest, Hungary
[25]*Korea University, Seoul, 136-701, Korea*
[26]*Russian Research Center "Kurchatov Institute," Moscow, Russia*
[27]*Kyoto University, Kyoto 606-8502, Japan*
[28]*Laboratoire Leprince-Ringuet, Ecole Polytechnique, CNRS-IN2P3, Route de Saclay, F-91128 Palaiseau, France*
[29]*Lawrence Livermore National Laboratory, Livermore, California 94550, USA*
[30]*Los Alamos National Laboratory, Los Alamos, New Mexico 87545, USA*
[31]*LPC, Université Blaise Pascal, CNRS-IN2P3, Clermont-Fd, 63177 Aubiere Cedex, France*
[32]*Department of Physics, Lund University, Box 118, SE-221 00 Lund, Sweden*
[33]*Institut für Kernphysik, University of Muenster, D-48149 Muenster, Germany*
[34]*Myongji University, Yongin, Kyonggido 449-728, Korea*
[35]*Nagasaki Institute of Applied Science, Nagasaki-shi, Nagasaki 851-0193, Japan*
[36]*University of New Mexico, Albuquerque, New Mexico 87131, USA*
[37]*New Mexico State University, Las Cruces, New Mexico 88003, USA*
[38]*Oak Ridge National Laboratory, Oak Ridge, Tennessee 37831, USA*
[39]*IPN-Orsay, Universite Paris Sud, CNRS-IN2P3, BP 1, F-91406 Orsay, France*
[40]*Peking University, Beijing, People's Republic of China*
[41]*PNPI, Petersburg Nuclear Physics Institute, Gatchina, Leningrad region, 188300, Russia*
[42]*RIKEN, The Institute of Physical and Chemical Research, Wako, Saitama 351-0198, Japan*
[43]*RIKEN BNL Research Center, Brookhaven National Laboratory, Upton, New York 11973-5000, USA*
[44]*Physics Department, Rikkyo University, 3-34-1 Nishi-Ikebukuro, Toshima, Tokyo 171-8501, Japan*
[45]*Saint Petersburg State Polytechnic University, St. Petersburg, Russia*
[46]*Universidade de São Paulo, Instituto de Física, Caixa Postal 66318, São Paulo CEP05315-970, Brazil*
[47]*System Electronics Laboratory, Seoul National University, Seoul, South Korea*
[48]*Chemistry Department, Stony Brook University, Stony Brook, SUNY, New York 11794-3400, USA*
[49]*Department of Physics and Astronomy, Stony Brook University, SUNY, Stony Brook, New York 11794, USA*
[50]*SUBATECH (Ecole des Mines de Nantes, CNRS-IN2P3, Université de Nantes) BP 20722, 44307 Nantes, France*
[51]*University of Tennessee, Knoxville, Tennessee 37996, USA*
[52]*Department of Physics, Tokyo Institute of Technology, Oh-okayama, Meguro, Tokyo 152-8551, Japan*
[53]*Institute of Physics, University of Tsukuba, Tsukuba, Ibaraki 305, Japan*
[54]*Vanderbilt University, Nashville, Tennessee 37235, USA*
[55]*Waseda University, Advanced Research Institute for Science and Engineering, 17 Kikui-cho, Shinjuku-ku, Tokyo 162-0044, Japan*

[56]Weizmann Institute, Rehovot 76100, Israel
[57]Yonsei University, IPAP, Seoul 120-749, Korea
(Received 12 November 2006; published 8 June 2007)

J/ψ production in $p + p$ collisions at $\sqrt{s} = 200$ GeV has been measured by the PHENIX experiment at the BNL Relativistic Heavy Ion Collider over a rapidity range of $-2.2 < y < 2.2$ and a transverse momentum range of $0 < p_T < 9$ GeV/c. The size of the present data set allows a detailed measurement of both the p_T and the rapidity distributions and is sufficient to constrain production models. The total cross section times the branching ratio is $B_{ll}\sigma_{pp}^{J/\psi} = 178 \pm 3^{\text{stat}} \pm 53^{\text{sys}} \pm 18^{\text{norm}}$ nb.

DOI: 10.1103/PhysRevLett.98.232002 PACS numbers: 13.85.Ni, 13.20.Fc, 14.40.Gx, 25.75.Dw

J/ψ mesons are produced in hadronic collisions involving hard processes that proceed primarily through diagrams involving gluons, such as gluon-gluon fusion. Once the $c\bar{c}$ pair is produced, it must evolve through a hadronization process to form a physical J/ψ meson. While this production has been extensively studied, the details of the production mechanism and hadronization remain an open question. Attempts at a consistent theoretical description of J/ψ meson production have been made, but it has proven difficult to reproduce both the observed cross sections and the polarization [1–4]. An additional complication is that nearly 30%–40% of the measured J/ψ meson yield results from feeddown of higher mass states (ψ', χ_c) [5] which reduces the observed polarization with respect to that expected from directly produced J/ψ mesons.

The color-singlet model [6], which generates a color-singlet $c\bar{c}$ pair in the same quantum state as the J/ψ meson, underpredicts the measured J/ψ cross section by approximately an order of magnitude [2]. Alternatively, the color-octet model includes color-octet $c\bar{c}$ pairs that radiate soft gluons during J/ψ meson formation [7]. However, the predicted transverse J/ψ polarization at high p_T is not seen in the data [2,4], and the color-octet matrix elements are not universal [8]. The color evaporation model, a more phenomenological approach, forms the different charmonium states in proportions determined from experimental data for any $c\bar{c}$ pair with a mass below the $D\bar{D}$ threshold and predicts no polarization. Finally, a recent perturbative QCD calculation including 3-gluon diagrams is able to successfully reproduce both the observed cross section and the polarization results [9].

A fundamental understanding of the J/ψ production process is also critical for defining the configuration of the produced $c\bar{c}$ state. This will have direct implications on the interaction of this state both with cold nuclear matter in proton or deuteron-nucleus collisions and with the high-density partonic matter observed in high-energy heavy-ion collisions. High quality experimental results over a wide kinematic range and collision energies are required to constrain models and to provide an improved understanding of J/ψ (and other heavy quarkonia) production.

In this Letter, J/ψ production in $p + p$ collisions at $\sqrt{s} = 200$ GeV measured by the PHENIX experiment at the BNL Relativistic Heavy Ion Collider (RHIC) is reported. The J/ψ cross section and transverse momentum distributions are studied in the mid ($|y| \leq 0.35$) and forward ($1.2 < |y| < 2.2$) rapidity regions. The data presented were collected during the 2005 RHIC run and exceed by more than 1 order of magnitude the previously reported number of J/ψ mesons [10,11].

At midrapidity, the PHENIX [12] drift chambers (DC), ring imaging Čerenkov detectors (RICH), and electromagnetic calorimeters (EMCal) are used to detect $J/\psi \rightarrow e^+e^-$ decays in two arms, each covering $\Delta\phi = 90°$ in azimuth. The muon detectors, consisting of cathode strip tracking chambers in a magnetic field (MuTr) and alternating layers of steel absorber and Iarocci tube planes (MuID), are used to measure $J/\psi \rightarrow \mu^+\mu^-$ at forward and backward rapidities over $\Delta\phi = 360°$.

The data were recorded using a minimum bias trigger that requires at least one hit in each of the beam-beam counters (BBCs) at forward and backward rapidities, $3.0 < |\eta| < 3.9$. Dielectron events must pass an additional trigger that consists of a logical OR between the level-1 electron and photon triggers. This trigger requires matching hits between the EMCal and RICH in a small angular area with a minimum energy deposition of 0.4 GeV in any 2×2 patch of EMCal towers. The photon trigger requires a minimum energy deposition of 1.4 GeV in any 4×4 set of overlapping EMCal towers. A trigger efficiency of 96% was achieved within the collision vertex range $|z_{\text{vtx}}| < 30$ cm for J/ψ candidates. Dimuon triggered events were selected using an online level-1 trigger that requires at least two particles penetrate the MuID. One particle must penetrate the entire MuID, while the second has a minimum penetration depth of 3 out of the 5 pairs of detector and absorber planes. Approximately 92% of the J/ψ mesons in events that satisfy the $|z_{\text{vtx}}| < 30$ cm cut fulfill this requirement. As part of the reconstruction chain, a level-2 filter is applied, consisting of a fast reconstruction of the particle trajectory in the MuTr and MuID. Events are accepted by this filter when at least two particles penetrate the entire MuID and have a reconstructed invariant mass ≥ 2.0 GeV/c^2. After applying cuts on the collision vertex position and quality assurance criteria, the sampled statistics corresponds to 2.6 pb^{-1} in the dielectron analysis, 2.7 pb^{-1} in the muon arm covering $1.2 < y < 2.2$, and 3.5 pb^{-1} in the muon arm covering $-2.2 < y < -1.2$.

At midrapidity, electron candidates are charged tracks associated with at least two hit phototubes in the RICH and one EMCal hit with a position matching of ± 4 standard

deviations (σ). The energy-momentum matching requirement is $(E/p - 1) \geq -4.0\sigma$. The number of J/ψ candidates is obtained by counting the unlike-sign dielectron pairs in a fixed mass window after subtracting the like-sign pairs. Figure 1(a) shows the invariant mass spectrum for dielectron pairs after subtracting the like-sign background. The mass window for counting the J/ψ signal is 2.7–3.5 or 2.6–3.6 GeV/c^2 depending on the number of DC hits used to reconstruct each track. The solid line in the figure is the sum of the J/ψ line shape (dashed curve) and an exponential function (dotted-dashed curve) describing the continuum component. The J/ψ line shape function accounts for detector resolution, internal radiative effects [13], and external radiative effects evaluated using a GEANT [14] simulation of the PHENIX detector. The J/ψ counts are corrected for the continuum yield, which originates primarily from open charm pairs and Drell-Yan processes inside the mass window (10% ± 5%), and the fraction of J/ψ candidates outside of the mass window (7.2% ± 1.0%). Approximately 1500 $J/\psi \rightarrow e^+e^-$ are obtained.

Muon track candidates are selected based upon their penetration depth in the MuID and the reconstructed track quality within the MuID and MuTr. The particle trajectory must contain at least 8 of 10 possible hits in the MuID, and the position matching between the MuID and MuTr must be within 15 (20) cm at positive (negative) rapidity. The J/ψ yield is obtained from the unlike-sign dimuon invariant mass distribution by subtracting the combinatorial background estimated using an event mixing technique. Three methods, shown in Fig. 1(b), are used to extract the J/ψ yield. Single Gaussian + exponential and double Gaussian + exponential functions are used to fit the J/ψ peak, while the contribution from the physical continuum and background is estimated using an exponential fit. The reported number of J/ψ mesons represents the average of the fit values. A total of 8000 $J/\psi \rightarrow \mu^+\mu^-$ are obtained.

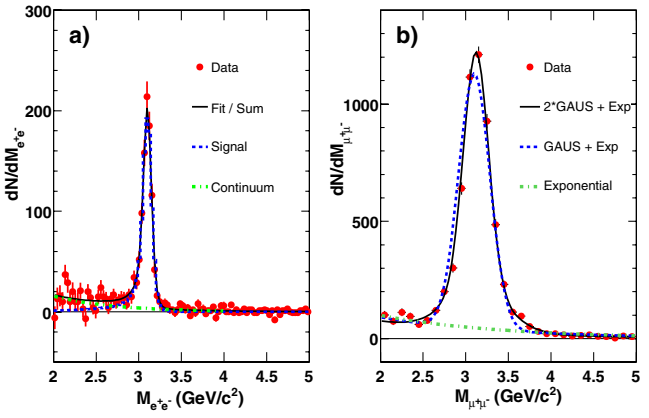

FIG. 1 (color online). Invariant mass spectra for (a) $J/\psi \rightarrow e^+e^-$ at $|y| < 0.35$ and (b) $J/\psi \rightarrow \mu^+\mu^-$ at $1.2 < |y| < 2.2$ with the functional forms used to extract the number of reconstructed J/ψ mesons.

The systematic uncertainty associated with the signal extraction is estimated from the variation between the fits.

The J/ψ cross section in a given rapidity and transverse momentum bin is calculated according to

$$\frac{B_{ll}}{2\pi p_T}\frac{d^2\sigma_{J/\psi}}{dydp_T} = \frac{1}{2\pi p_T \Delta p_T \Delta y}\frac{N_{J/\psi}}{\mathcal{L} A\epsilon_{\rm rec}\epsilon_{\rm trig}\epsilon^{\rm BBC}_{J/\psi}},$$

where B_{ll} is the J/ψ dilepton branching ratio, $N_{J/\psi}$ is the measured J/ψ yield, $\mathcal{L}$ is the integrated luminosity recorded by the minimum bias trigger, $A\epsilon_{\rm rec}$ represents the geometric acceptance and reconstruction efficiency, and $\epsilon_{\rm trig}$ is the trigger efficiency. $\epsilon^{\rm BBC}_{J/\psi}$ is the minimum bias trigger efficiency for events containing a J/ψ meson and was determined to be 0.79 ± 0.02 [10]. The cross section sampled by the BBC trigger, $\sigma^{pp}_{\rm tot} \times \epsilon^{\rm BBC}_{\rm MB} = 23.0 \pm 2.2$ mb, was used to determine the integrated luminosity.

The $A\epsilon_{\rm rec}$ and $\epsilon_{\rm trig}$ terms are determined individually for the central arm and each muon arm based upon the detection of simulated J/ψ mesons processed using the real data analysis chain. Decay events are generated and propagated through a full GEANT simulation of the detector, which includes the specific details of the detector performance including the MuTr and MuID alignment, disabled anodes, and MuID efficiency. Corrections were determined from the single electron yields for the dielectron analysis to account for the detector dead channel map, energy calibration, and run-to-run variations in the detector active area. The J/ψ trigger efficiency is incorporated via a level-1 trigger emulator tuned to describe the experimental trigger response. For the dimuon analysis, the level-2 filtering algorithms are applied to the simulated events. After reconstruction, the number of detected J/ψ mesons is compared to the number of simulated J/ψ mesons in a given rapidity and transverse momentum bin to determine the appropriate correction factors.

The systematic uncertainty associated with the measurement of the J/ψ cross section can be divided into three categories based upon the effect each source has on the measured results. All uncertainties are reported as standard deviations. Point-to-point uncorrelated uncertainties allow the data points to move independently with respect to one another. These include the signal extraction systematic, which is bin-dependent with typical values of 4% (5%) in the dimuon (dielectron) data, and the 1.5% J/ψ momentum smearing effect in the dielectron acceptance measurement. Point-to-point correlated uncertainties allow the data points to move coherently within the quoted value. Their values amount to 10% (8%) for the detector acceptance, 8% (4%) for the run-to-run variation in the detector efficiency, 4% (2.5%) for the J/ψ meson transverse momentum and vertex distributions, and 2% (2%) for the hardware efficiency of the detector. Finally, the global systematic uncertainty allows the data points to move together. The dominant source of this uncertainty originates from the estimation of the BBC triggering efficiency

for minimum bias events 9.7%, with an additional contribution from the uncertainty in the estimation of the number of sampled minimum bias events 1% and $\epsilon_{J/\psi}^{\mathrm{BBC}}$ 2.5%.

Figure 2(a) shows the transverse momentum spectra at both mid and forward rapidities, which are fit with the function $A \times [1 + (p_T/B)^2]^{-6}$ [15] to extract the value of the $\langle p_T^2 \rangle$. At midrapidity, the $\langle p_T^2 \rangle$ is $4.14 \pm 0.18 \pm^{0.30}_{0.20}$ $(\mathrm{GeV}/c)^2$, and the χ^2 per degree of freedom (χ^2/ndf) is 23/19. At forward rapidity, the $\langle p_T^2 \rangle$ is $3.59 \pm 0.06 \pm 0.16$ $(\mathrm{GeV}/c)^2$, and the χ^2/ndf is 28/17. The first error is statistical, and the second includes the systematic uncertainty from the maximum shape deviation permitted by the point-to-point correlated errors and from allowing the exponent of the fit function to be a free parameter. The statistical precision of the data is sufficient to allow the $\langle p_T^2 \rangle$ to be calculated directly from the numerical integration of the data. This calculation results in a $\langle p_T^2 \rangle$ of $4.25 \pm 0.24 \pm 0.14$ $(\mathrm{GeV}/c)^2$ at midrapidity and $3.57 \pm 0.06 \pm 0.15$ $(\mathrm{GeV}/c)^2$ at forward rapidity. Although good agreement is found with the rapidity distribution and total cross section, previously published results [11] yielded a significantly lower $\langle p_T^2 \rangle$ at forward rapidity than found here, even accounting for the quoted statistical and systematic uncertainties. The increased sample size of the present data set allows for an improved understanding of the shape of the p_T spectrum at forward rapidity due to the extended range in p_T and the finer binning at low p_T. The previous results have been revisited, and it was found that the systematic uncertainty was underestimated.

Figure 2(b) shows the ratio of the differential cross section times dilepton branching ratio at forward and midrapidity. The ratio falls with p_T and reaches a minimum of 0.5 above a p_T of 2 GeV/c. Although the present data are limited by significant systematic uncertainties, the data suggest that the forward rapidity p_T distribution is softer than at midrapidity. Such behavior could be attributed to an increase in the longitudinal momentum at forward rapidity leaving less energy available in the transverse direction.

The observed p_T distributions are substantially harder than those for lower energy $p + p$ and $p + A$ collisions as expected from the increased phase space at higher energy. Figure 3 shows the energy dependence of the average $\langle p_T^2 \rangle$ including points from the CERN Super Proton Synchrotron, Fermilab fixed target, and Tevatron measurements. A linear fit versus the log of the center of mass energy describes the general trend, although some variation is expected due to the differing rapidity ranges of the measurements and the use of $p + A$ data for some of the points.

Figure 4 shows the J/ψ differential cross section versus rapidity. The statistical precision of these results is sufficient to allow the data to be divided into 11 rapidity bins compared to the 5 bins used in the previous measurement [11]. Also shown are several models fit to the data. The dashed curve is a nonrelativistic QCD calculation [16]. The dotted-dashed curve is a pQCD calculation that includes diagrams describing a third gluon [9]. This model fails to reproduce the steeply falling cross section observed in the present data at large rapidity. An empirical double Gaussian fit (dotted-dotted curve) is able to reproduce the data best but has no theoretical foundation. The data slightly favor a flatter distribution over the rapidity range $|y| < 1.5$ than most models, but since the systematic error on the mid and forward rapidity points are independent, a narrower distribution is not excluded.

To determine the total cross section, the rapidity distribution was fit with many theoretical and phenomenological shapes including those shown in Fig. 4. A total cross section times the branching ratio of $B_{ll}\sigma_{pp}^{J/\psi} = 178 \pm 3^{\mathrm{stat}} \pm 53^{\mathrm{sys}} \pm 18^{\mathrm{norm}}$ nb is obtained from the fit that pro-

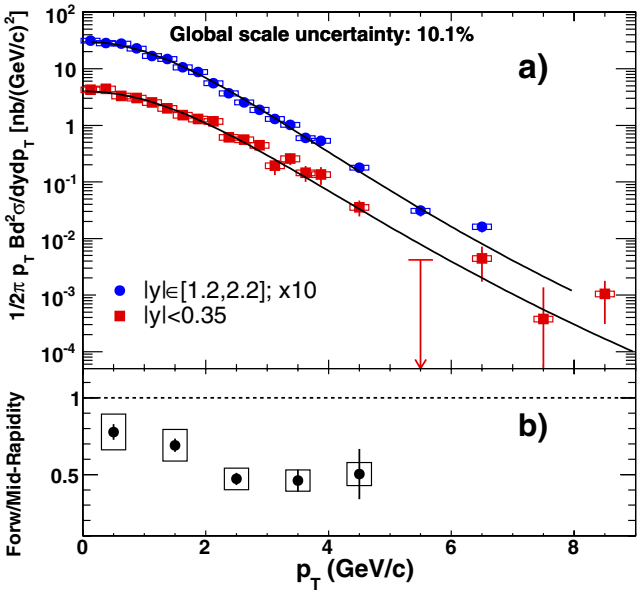

FIG. 2 (color online). (a) The forward rapidity (circles) and midrapidity (squares) J/ψ meson differential cross section times the dilepton branching ratio versus p_T and (b) the ratio of the forward and midrapidity p_T spectra.

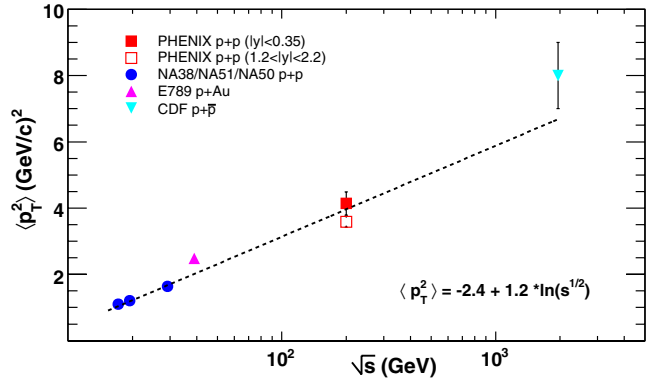

FIG. 3 (color online). PHENIX $\langle p_T^2 \rangle$ measurements compared to measurements at other energies [2,4,19] as a function of collision energy for J/ψ meson production in $p + p$ or $p + A$ collisions.

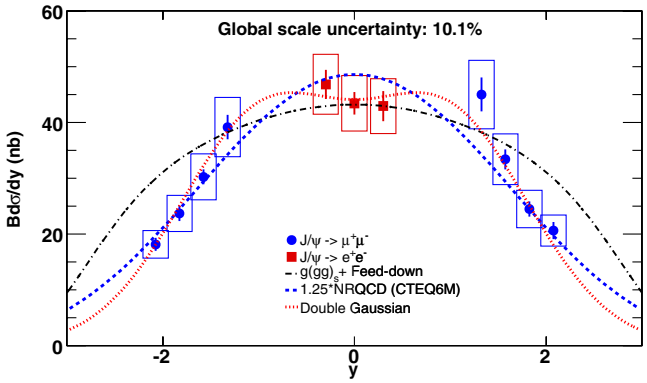

FIG. 4 (color online). The J/ψ differential cross section times the dilepton branching ratio plotted versus rapidity.

vides the best χ^2/ndf, double Gaussian. The absolute normalization error (norm) represents the uncertainty in the BBC trigger cross section. The systematic uncertainty (sys) is estimated by refitting the data with the same theoretical and phenomenological curves while simultaneously allowing the maximum variation in the shape of the distribution by shifting the mid and forward rapidity data independently by their point-to-point correlated systematic errors. Using the double Gaussian fit, the acceptance of the PHENIX data covers 92.1% of the integrated cross section. This result is consistent with our previous measurement [11].

We have presented J/ψ results for $p + p$ collisions at $\sqrt{s} = 200$ GeV that extend the reach in transverse momentum to 9 GeV/c. The measured p_T spectrum is harder than that observed at lower energies. The rapidity shape falls steeply at forward rapidity and cannot be reproduced by the pQCD calculation in Ref. [9]. Futhermore, the data slightly favor a flatter rapidity distribution than most models, but a narrower distribution is not excluded. These data not only constrain production models for heavy quarkonia but also provide a critical baseline for similar studies in deuteron-nucleus and heavy-ion collisions [11,17,18].

We thank the staff of the Collider-Accelerator and Physics Departments at BNL for their vital contributions. We acknowledge support from the Office of NP in DOE Office of Science and NSF (USA), MEXT and JSPS (Japan), CNPq and FAPESP (Brazil), NSFC (China), MSMT (Czech Republic), IN2P3/CNRS and CEA (France), BMBF, DAAD, and AvH (Germany), OTKA (Hungary), DAE (India), ISF (Israel), KRF and KOSEF (Korea), MES, RAS, and FAAE (Russia), VR and KAW (Sweden), U.S. CRDF for the FSU, U.S.–Hungarian NSF-OTKA-MTA, and U.S.–Israel BSF.

*Deceased.
†PHENIX Spokesperson.
Electronic address: zajc@nevis.columbia.edu

[1] M. Beneke, arXiv:hep-ph/9703429.
[2] F. Abe *et al.*, Phys. Rev. Lett. **69**, 3704 (1992); S. Abachi *et al.*, Phys. Lett. B **370**, 239 (1996); B. Abbot *et al.*, Phys. Rev. Lett. **82**, 35 (1999); F. Abe *et al.*, Phys. Rev. D **66**, 092001 (2002); D. Acosta *et al.*, Phys. Rev. D **71**, 032001 (2005). The $\langle p_T^2 \rangle$ was extracted using a fit of the form $A \times [1 + (p_T/B)^2]^{-6}$.
[3] R. Vogt, Phys. Rep. **310**, 197 (1999).
[4] M. H. Schub *et al.*, Phys. Rev. D **52**, 1307 (1995).
[5] I. Abt *et al.*, Phys. Lett. B **561**, 61 (2003).
[6] E. L. Berger and D. Jones, Phys. Rev. D **23**, 1521 (1981); R. Baier *et al.*, Phys. Lett. **102B**, 364 (1981).
[7] G. T. Bodwin, E. Braaten, and G. P. Lepage, Phys. Rev. D **51**, 1125 (1995); **55**, 5853(E) (1997).
[8] J. K. Mizukoshi, arXiv:hep-ph/9911384.
[9] V. A. Khoze *et al.*, Eur. Phys. J. C **39**, 163 (2005); (private communication).
[10] S. S. Adler *et al.*, Phys. Rev. Lett. **92**, 051802 (2004).
[11] S. S. Adler *et al.*, Phys. Rev. Lett. **96**, 012304 (2006).
[12] K. Adcox *et al.*, Nucl. Instrum. Methods Phys. Res., Sect. A **499**, 469 (2003).
[13] A. Spiridonov, arXiv:hep-ex/0510076.
[14] GEANT 3.2.1, CERN Computing Library, http://wwwasd.web.cern.ch/wwwasd/geant/index.html.
[15] J. K. Yoh *et al.*, Phys. Rev. Lett. **41**, 684 (1978); (private communication).
[16] F. Cooper, M. X. Liu, and G. C. Nayak, Phys. Rev. Lett. **93**, 171801 (2004); (private communication).
[17] A. Adare *et al.*, following Letter, Phys. Rev. Lett. **98**, 232301 (2007).
[18] A. Adare *et al.* (to be published).
[19] O. Drapier, Thèse d'habilitation thesis, Université Claude Bernard-Lyon, 1998, http://na50.web.cern.ch/NA50/theses.html.